ISBN: 978-981-18-5852-9
WCSE 2022 Spring Event: 2022 9th International Conference on Industrial Engineering and Applications
doi: 10.18178/wcse.2022.04.121

Numerical Investigation on Crashworthiness of Fiber Braided Composites Subjected to Oblique Hypervelocity Impact

Mingyu Cai [1], Dahai Zhang [1], Song Wu [2,3] and Qingguo Fei [1]

[1] School of Mechanical Engineering Southeast University

[2] Department of Aeronautics and Astronautics Fudan University

[3] Shanghai Aerospace System Engineering Research Institute

Abstract. The impact damage and crashworthiness of flexible braided composite structures were numerically evaluated by means of the finite element (FEM) and smoothed particle hydrodynamics (SPH) method. Numerical models of the fiber braided composite considering micro structures were constructed and validated by comparing simulation results with experiments. Specifically, effect of the impact angle on behaviors of the flexible braided composites were analyzed. Results show that the FEM-SPH models could effectively simulate failure and perforation of the braided composite structure. Impact angle could affect the crashworthiness and damage characteristics of the composites significantly. The shape and size variation of debris cloud under different impact angles are obtained. With the increase of impact angle, from the perforation of the shields and the absorption of the projectile kinetic energy, the damage ability of projectile to the shield increases first and then decreases.

Keywords: hypervelocity impact, fiber braided composite, oblique impact, FEM-SPH.

1. Introduction

A large number of space debris and micrometeoroids exist in the space environment, which seriously threaten the normal on-orbit operation of spacecraft or space station cabin and the life safety of astronauts[1]. Therefore, it is of great significance to improve the safety, stability and prolong the life of spacecraft by protecting the structure weakening or avoiding the damage caused by hypervelocity impact.

In 1947, Whipple proposed Whipple shield[2], which was composed of two homogeneous metal plates as front and rear plates separated by a distance, in order to avoid the direct damage of spacecraft subjected to hypervelocity impact. With the development of space technology, space structures are becoming larger and lighter. Flexible braided materials have the advantages of foldable expansion and can be used for inflatable space capsules[3]. They have the advantages of small envelope volume, large internal space and relatively light weight, which effectively make up for the shortcomings of traditional space structures.

The vertical hypervelocity impact problem has been extensively studied by researchers from all over the world, but the statistics show that most of the impact of space debris on the surface of the spacecraft is an oblique impact rather than a vertical impact[4]. So far, there is relatively little research work on oblique impact. When studying the hypervelocity impact characteristics of space debris protection structures, oblique impact must be regarded as a common phenomenon. The current research on the hypervelocity impact characteristics of the research parameters is mainly based on the size of the perforation[5], there are also studies on the characteristic size of the debris cloud. Zhang conducted a hypervelocity impact test on the double-shield aluminum structure, and fitted the empirical formula of the perforation size according to the impact speed, angle, thickness of the shield and other parameters[6]. Liu analyzed the perforation characteristics of aluminum alloy thin plate under hypervelocity oblique impact and the characteristics of projectile fragment cloud, and established the perforation empirical formula of aluminum alloy spherical projectile under hypervelocity oblique impact on aluminum alloy thin plate[7]. Nasit proposed a debris distribution model of oblique impact, which is in good agreement with the experiment[8]. Schonberg established a model to predict the spread and trajectory of ricochet debris particles created in a hypervelocity impact as well as the size and velocity of the most damage particle in the ricochet debris cloud[9]. In the study of hypervelocity oblique impact, the target plate mainly uses metal materials, such as aluminum alloy [10],[11], there are relatively few studies on composites[12],[13].

In this paper, the hypervelocity impact model is established based on the Finite Element Method (FEM) and Smooth Particle Hydrodynamics (SPH). The oblique hypervelocity impact numerical simulation of the fiber braided shield is carried out under different impact angles. The shape and size of the fragment cloud, the perforation damage of the shield and the change law of the kinetic energy of the projectile under different impact angles are obtained.

2. Simulation Methodology

2.1. Projectile Model

The projectile material used is aluminum alloy. In order to describe the state of aluminum alloy during hypervelocity impact, the Mie-Gruneisen equation is used to describe:

$$p - p_{\mathrm{H}} = \Gamma\rho(E_{\mathrm{m}} - E_{\mathrm{H}}) \tag{1}$$

where $\Gamma=\Gamma_0\rho_0/\rho$, E_{m} is the internal energy per unit mass, p_{H} and E_{H} represent Hugoniot pressure and specific energy per unit mass, respectively. And:

$$p_{\mathrm{H}} = \frac{p_0 c_0^2 \mu(1+\mu)}{[1-(s-1)\mu]^2} \tag{2}$$

$$E_{\mathrm{H}} = \frac{1}{2}\frac{p_{\mathrm{H}}}{p_0}\left(\frac{\mu}{1+\mu}\right) \tag{3}$$

where $\mu=\rho/\rho_0$-1, ρ represents the density at different temperatures, ρ_0 represents the initial density, and c_0 is the speed of sound in the initial state. In the equation of state of aluminum alloy, Γ_0, s and c_0 are taken as 2.0, 1.338 and 5328 m/s, respectively. The specific heat capacity of aluminum alloy is 921 J/(kg·°C).

The material will deform strongly under hypervelocity impact accompanied by higher strain rate and temperature. In order to better describe this characteristic, the Johnson-Cook model is used to describe the deformation behavior of aluminum alloy. In this model, the yield stress of the material σ_y varies according to strain, strain rate and temperature:

$$\sigma_y = \left[A + B\varepsilon_{\mathrm{p}}^n\right]\left[1 + C\ln\varepsilon_{\mathrm{p}}^*\right]\left[1 - T_{\mathrm{H}}^m\right] \tag{4}$$

$$T_{\mathrm{H}} = (T - T_{\mathrm{room}})/(T_{\mathrm{melt}} - T_{\mathrm{room}}) \tag{5}$$

where ε_{p} is the effective plastic strain, $\varepsilon_{\mathrm{p}}^*$is the effective plastic strain rate, T_{room} is room temperature, T_{melt} is the melting temperature, A is the initial yield stress, B is the hardening constant, C is the strain rate constant, and m is the thermal softening exponent, n is the strain hardening exponent. The specific parameters of the projectile model material are shown in Table 1.

Table 1: material parameters of the projectile

Parameter	Initial Yield Stress /MPa	Hardening Constant /MPa	Strain Rate Constant	Thermal Softening Exponent	Hardening Exponent	Melting Temperature /°C
Value	265	426	0.015	1	0.34	591

The shape of the projectile is spherical. In the numerical simulation, the projectile is modeled by solid elements, and it is transformed into particles at the beginning of the analysis. The distance between particles is 0.2 mm.

2.2. Fiber Woven Material Model

The research on the hypervelocity impact of traditional flexible braided materials usually adopts equivalent modeling method, which is mainly suitable for the simulation of homogeneous materials such as metal plates. If a flexible woven material is modeled using a homogeneous method, it will not be able to reflect the interaction and deformation mechanism of the yarn in the fabric under impact load, which will seriously affect the accuracy of the analysis. Therefore, when analyzing the hypervelocity impact of flexible braided materials, it is necessary to carry out micro modeling. The fiber woven material is woven by transverse and longitudinal fiber bundles, which are modeled by two-dimensional weaving, and the woven fabric structure is formed by interactive weaving between warp yarns and weft yarns. By changing the geometric parameters of the woven material unit cell model, woven materials with different areal densities can be established. The woven material mesh model established by this modeling method is shown in Fig. 1.

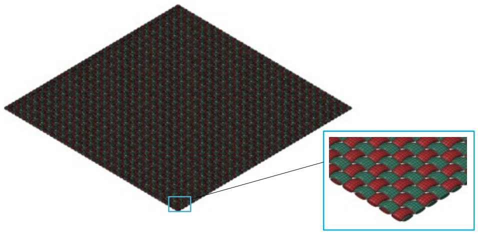

Fig. 1: The grid model of the braided material

The orthotropic constitutive is used to describe the fiber woven material. Establish a local coordinate system for fiber bundles in the same direction, the x-axis is consistent with the fiber direction, the y-axis is perpendicular to the x-axis and in the same fiber plane as the x-axis, and the z-axis is a right-hand rule with the other two axes. The elastic modulus E1 along the fiber direction is much larger than the elastic modulus E2, E3 and the shear modulus G12, G23, G31 perpendicular to the fiber direction. The material parameters of the aramid fiber used in this paper are shown in Table 2.

Table 2: material parameters of the fiber braided material

Parameter	Density /($g\cdot cm^{-3}$)	Elastic Modulus E_1/GPa	Elastic Modulus E_2/GPa	Elastic Modulus E_3/GPa	Poisson's Ratio ν_{12}	Poisson's Ratio ν_{23}	Poisson's Ratio ν_{31}	Shear Modulus G_{12}/GPa	Shear Modulus G_{23}/GPa	Shear Modulus G_{31}/GPa	Failure Strain ε	Failure Stress σ/GPa
Value	1.44	164	3.28	3.28	0.01	0.01	0.01	3.28	3.28	3.28	0.045	3.88

2.3. Numerical Simulation Method Verification

In order to verify the fiber woven material modeling method and its hypervelocity impact perforation damage characteristics, the experiments in the literature are used for numerical simulation and comparative verification[14]. The model size and structural material parameters adopt the data in the literature. The diameter of projectile in the experiment is 3.97 mm, the speed is 3.9 km/s, the projectile material is aluminum alloy, the shield material is aramid, and the areal density is 350 g/m2. The numerical simulation results are shown in Fig. 2. The figure shows that the front perforation diameter of the protection structure obtained by the numerical simulation is 4.49 mm, the experimental result in the literature is 5.3 mm, the relative error is 15.28%, and the back perforation diameter obtained by the numerical simulation is 7.46 mm. The experimental result in the literature is 7.9 mm, and the relative error is 5.57%. Because the influence of temperature on the woven material under hypervelocity impact is not considered, the perforation diameter is smaller than the experimental result, but the error is within a certain range, which can effectively simulate the perforation characteristics of the fiber woven material.

Experimental results

Simulation results

Fig. 2: Numerical simulation of fabric perforation validation results

In summary, the projectile and fiber woven material simulation method used in this paper can effectively simulate the hypervelocity impact damage and characteristics of the fiber woven material.

3. Results and Discussion

The hypervelocity impact characteristic analysis model is shown in Fig. 3. The diameter of the projectile selected by the numerical simulation is 3 mm, the impact velocity is 1.5 km/s and the boundary condition of the shield is the surrounding fixed support. The impact angle is the angle between the impact direction of the projectile and the normal direction of the impact surface of the shield. The flexible woven material shield is composed of eight layers of aramid fiber cloth with a density of 384 g/m2.

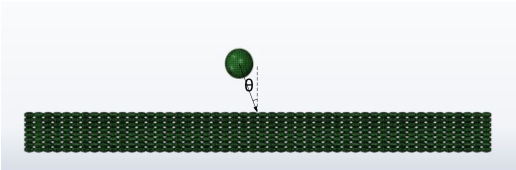

Fig. 3: The grid model of the shield with different angles

3.1. Debris Cloud Shape and Size

The shape of the debris cloud generated with different projectile impact angles is showed in Fig. 1. Geometric parameters are used to describe the characteristics of debris clouds. As shown in Fig. 2, L is the longitudinal spread distance, which represents the distance that the debris cloud spreads along the 0° direction at 40 μs. W is the transverse spread distance, which represents the distance that the debris cloud spreads along the 90° direction at 40 μs. As the impact angle increases, the debris cloud deflects toward the impact velocity direction. When the impact angle reaches 60°, the projectile fragments will splash back. A small number of projectile fragments will appear behind the shield, but most of the projectile fragments pass through the shield. When the impact angle reaches 75°, the fragments of the projectile will slide. The shield was not completely penetrated by the projectile, a small part of the fragments remained in the shield, and most of the projectile fragments slid. Fig. 6 shows the relationship between the spread distance of the debris cloud and the impact angle. As the impact angle increases, the longitudinal spread distance L of the debris cloud gradually decreases, and the transverse spread distance W first increases, then decreases and then increases. This is because when the impact angle gradually increases, the spread direction of the debris cloud deviates from the vertical line of the shield along the impact angle direction, so the longitudinal spread distance gradually decreases and the transverse spread distance will increase. When the impact velocity reaches 60 °, the fragments will splash back, and the spread in the transverse direction will be restrained, so the transverse spread distance decreases. When the impact angle continues to increase, the projectile fragments slide, which further aggravates the spread of projectile fragments in the transverse direction and the transverse spread distance increases.

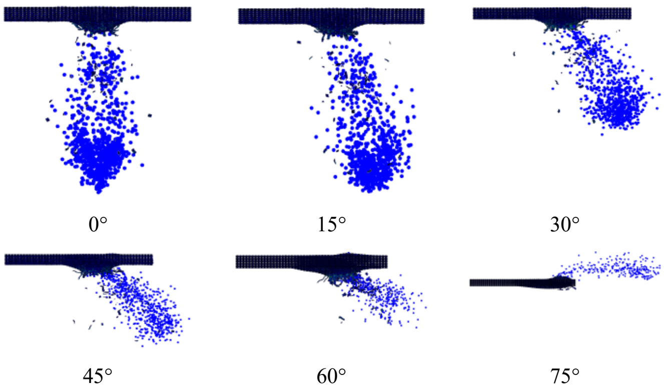

Fig. 1: Simulation results of different impact angles at 40μs

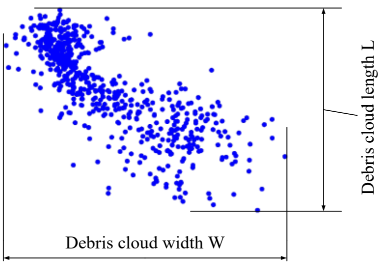

Fig. 2: Debris cloud characteristic parameters

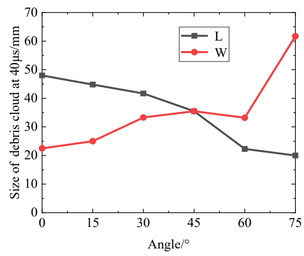

Fig. 3: Size of the debris cloud with different angles

3.2. Damage of the Shield

The damage of the shields with different impact angles is showed in Fig. 4. When the impact angle is less than 60°, the shield is completely penetrated, the fibers fall off, and the falling off direction is shifted toward the impact angle. When the impact angle was 75°, the projectile did not completely pass through the shield, and a large bulge appeared in the shield. When the projectile impacts the shield obliquely, oval perforation will occur on the shield. Since the shield is made of multiple layers of fiber cloth, the perforation size of each layer of fiber cloth is not the same. Fig. 5 shows the perforation of each layer of fiber cloth under different impact angles, from left to right are 1-8 layers of fiber cloth. Use the long axis of the perforated ellipse to quantitatively describe the damage to the fiber cloth. Fig. 6 is the graph showing the change of the long axis of the perforated ellipse of each layer of fiber cloth under different impact angles. When the impact angle is between 0° and 60°, the size of the long axis of the elliptical perforation of the fiber cloth increases from front to rear. This is because the projectile breaks more and more completely after passing through the fiber cloth, making the perforation of the fiber cloth in the rear layer larger and larger. Comparing the size of the long axis of the perforated ellipse of the same layer of fiber cloth under different impact angles, it can be found that when the impact angle is between 0° and 60°, the larger the impact angle is, the larger the long axis of the perforated ellipse is, because the larger the impact angle component in the long axis direction is, which is conducive to the increase of the long axis of the ellipse. When the impact angle increases to 75 °, the projectile slides, and the component of projectile velocity in the 0 ° direction becomes smaller. Only the first four layers of the protective structure penetrate, and the perforation of the second layer is the largest. The long axis of the perforation ellipse first increases and then decreases, and there is no perforation in the next four layers. Moreover, because of the slide of projectile fragments, the size of the long axis of the perforated ellipse is significantly larger than the size of the perforation without slide.

The kinetic energy absorption rate of the projectile is used to describe the protective effect of the shield on the hypervelocity impact of projectiles with different impact angles. From the results in Fig. 7, it can be analyzed that when the impact angle is between 0° and 75°, as the impact angle increases, the absorption rate of the kinetic energy of the projectile by the protective structure gradually increases, and the growth trend shows a slow rise, a sharp rise and then a slow rise trend. This is because when the impact angle is small, the projectile will not splash back, and the kinetic energy absorption rate of the projectile has a greater relationship with the damage area of the shield, resulting in a slow growth trend. When the impact angle increases, the shield has an inhibitory effect on the longitudinal and transverse spread of projectile fragments, and the kinetic energy absorption rate increases faster. When the impact angle continues to increase, due to the sliding of the projectile, the growth trend of the kinetic energy absorption rate drops again. When the impact angle continues to increase to 85 °, the sliding degree of the projectile increases, and the projectile kinetic energy is rarely absorbed by the shield.

4. Conclusion

The FEM-SPH models could effectively simulate failure and perforation of the braided composite structure. The impact angle has a great influence on the shape and size of debris cloud. In a certain range, the larger the impact angle, the larger the long axis of the perforation of the shield, and the greater the kinetic energy absorption rate of the projectile. However, when the impact angle continues to increase, the sliding degree of the projectile increases, and the damage ability of the projectile to the shield decreases.

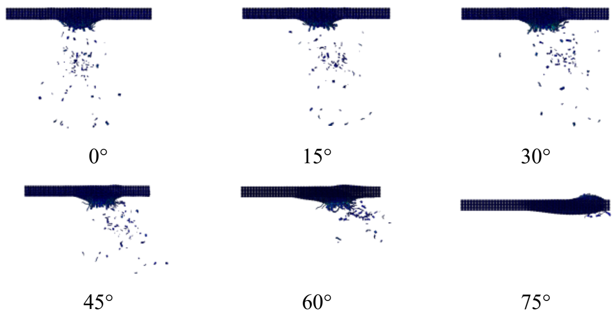

Fig. 4: Damage of the shields with different impact angle

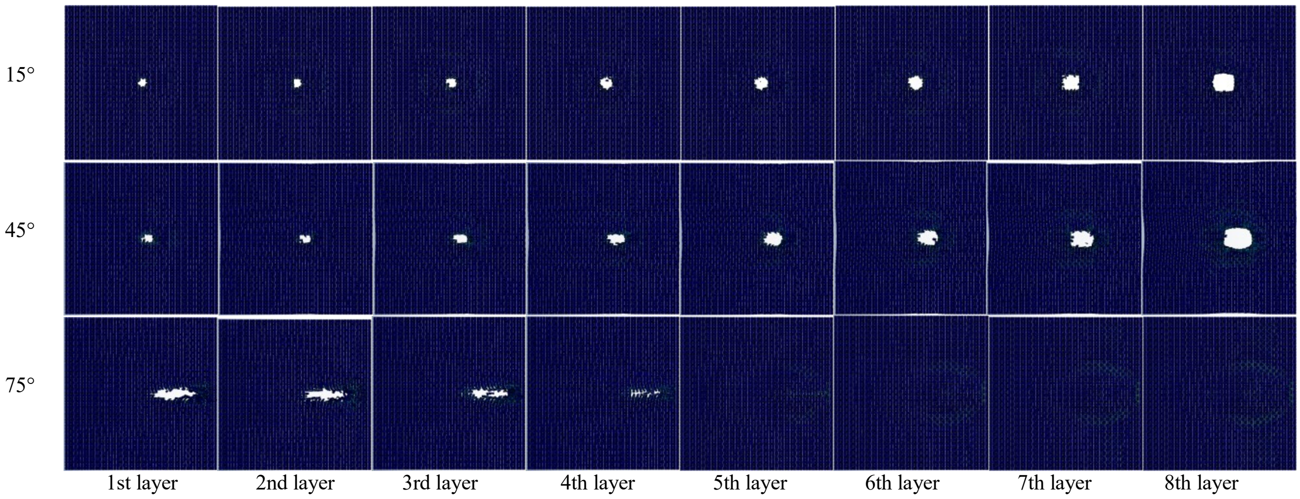

Fig. 5: Perforation of each layer of the shields with different impact angles

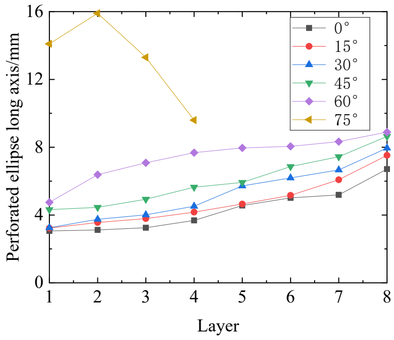

Fig. 6: Perforation size of different layers of fiber cloth with different impact angles

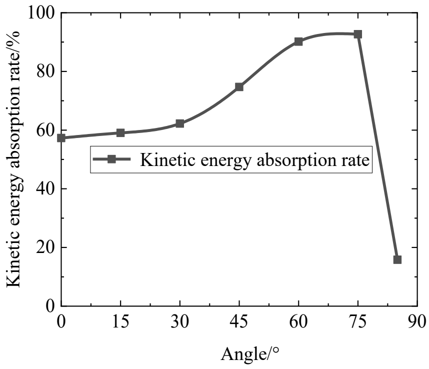

Fig. 7: Kinetic energy changes of projectiles with different impact angles

5. Acknowledgements

The research work is supported by the National Natural Science Foundation of China (52005100), the Jiangsu Natural Science Foundation (BK20190324), the Shanghai Space Science and Technology Innovation Fund (SAST2019-019), the Fundamental Research Funds for the Central Universities and Zhishan Youth Scholar Program of SEU (2242021R41169).

6. References

[1] Z. Z. Gong, Q. Y. Zhao and M. Li, "The frontier problem and prospect of space debris protection research," Space Debris Research, 19.3(2019):2-13.

[2] F. L. Whipple, "Meteorites and space travel" Astronomical Journal, 52.5(1947):131.

[3] A. Epb, A. Isk and B. Vvs, "Protection of inflatable modules of orbital stations against impacts of particles of space debris," Acta Astronautica, 163(2019):54-61.

[4] C. J. Ortega, "Highy oblique impacts into thick and thin targets," International Journal of Impact Engineering, 14.1(1993):157-168.

[5] K. D. Dhote and P. N. Verma, "Investigation of hole size formation by steel sphere impacting on thin plate at hypervelocity," Procedia Engineering, 173(2017): 323-330.

[6] Q. Zhang, Y. Chen and F. Huang, "Experimental study on expansion characteristics of debris clouds produced by oblique hypervelocity impact of LY12 aluminum projectiles with thin LY12 aluminum plates," International Journal of Impact Engineering, 2008, 35(12):1884-1891.

[7] X. Liu, Y. J. Deng, Y. Peng and Y. Yao, "Simulation analysis of the characteristics of debris cloud and perforation caused by oblique hypervelocity impact of spherical projectile on a thin plate," Space Craft Environment Engineering, 38.6(2021): 615-624.

[8] Nasit and J. S. Wilbeck, “Debris fragment characterization in oblique hypervelocity impacts,” International Journal of Impact Engineering, (1993).

[9] W. P. Schonberg, “Characterizing secondary debris impact ejecta,” International Journal of Impact Engineering, 26(2001):713-724.

[10] M. Nishida, K. Hayashi and K. Toya, “Influence of impact angle on size distribution of fragments in hypervelocity impacts,” International Journal of Impact Engineering, 128(2019):86-93.

[11] G. S. Guan, Y .Ha and B. J. Pang, “Investigation on Damage Characteristics of Thin Al-Plates by Oblique Hypervelocity Impact of Al-Sphere,” Chinese Journal of High Pressure Physics, 21.4(2007):7.